Spatial and temporal patterns in Arctic river ice breakup revealed by automated ice detection from MODIS imagery

Sarah W. Cooley *, Tamlin M. Pavelsky

Department of Geological Sciences, University of North Carolina at Chapel Hill, 104 South Rd, Chapel Hill, NC 27599, USA

A R T I C L E I N F O

Article history:
Received 26 May 2015
Received in revised form 20 November 2015
Accepted 7 January 2016
Available online 21 January 2016

Keywords:
River ice breakup
MODIS
Arctic hydrology
Climate change

A B S T R A C T

The annual spring breakup of river ice has important consequences for northern ecosystems and significant economic implications for Arctic industry and transportation. River ice breakup research is restricted by the sparse distribution of hydrological stations in the Arctic, where limited available data suggests a trend towards earlier ice breakup. The specific climatic mechanisms driving this trend, however, are complex and can vary both regionally and within river systems. Consequently, understanding the response of river ice processes to a warming Arctic requires simultaneous examination of spatial and temporal patterns in breakup timing. In this paper, we describe an automated algorithm for river ice breakup detection using MODIS satellite imagery that enables identification of spatial and temporal breakup patterns at large scales. We examine breakup timing on the Mackenzie, Lena, Ob' and Yenisey rivers for the period 2000–2014. By dividing the rivers into 10 km segments and classifying each river pixel in each segment as snow/ice, mixed ice/water or open water based on MODIS reflectance, we determine breakup dates with a mean uncertainty of ± 1.3 days. All statistically significant temporal trends are negative, indicating an overall shift towards earlier breakup. Considerable variability in the statistical significance and magnitude of trends along each river suggests that different climatic and physiographic drivers are impacting spatial patterns in breakup. Trends detected on the lower Mackenzie corroborate recent studies indicating weakening ice resistance and earlier breakup timing near the Mackenzie Delta. In Siberia, the increased magnitude of trends upstream and strong correlation between breakup initiation and whole-river breakup patterns suggest that earlier onset of upstream discharge may play the dominant role in determining breakup timing. Exploratory analysis demonstrates that MODIS imagery may also be used to differentiate thermal and mechanical breakup events.

1. Introduction

River ice formation and breakup are major events for the ecosystems and economies of the pan-Arctic region. Ice breakup substantially impacts regional transportation dependent on rivers, and corresponding ice jam floods can be devastating to bridge, dam and hydropower infrastructure. Peak flow occurs around the time of ice breakup on many rivers, and the combination of high velocity flow and floating ice is a potent erosive mechanism impacting the river banks and the surrounding landscape (Prowse, 2001a). Spring ice breakup can result in up to $250 million of damage in North America and more than $100 million in Russia every year (Beltaos & Prowse, 2009). While damages to human infrastructure can be substantial, river ice breakup is also an integral part of Arctic ecosystems. Hydrologic recharge from the resultant flooding is particularly important to the ecology of wetlands and ponds located near Arctic rivers (Prowse, 2001b), and the spring freshet mobilizes and transports large amounts of sediment and nutrients vital to the riparian life of the region (Prowse, 2001a).

Fundamentally, river ice breakup is controlled by the balance between the driving force (upstream discharge) and the resisting force (downstream ice cover) (Beltaos & Prowse, 2009). Breakup events can have substantially different characteristics depending on whether mechanical or thermal processes dominate. Mechanical breakup events are characterized by high discharge and limited downstream melting, often causing significant ice-jam flooding as relatively intact ice cover clogs the channel. In contrast, thermal breakup events occur when high temperatures and solar radiation substantially degrade the ice prior to the arrival of the spring freshet. Processes affecting ice resistance (e.g., insolation, surface air temperature, ice thickness) and discharge timing and magnitude (e.g., upstream air temperature, snowpack) produce breakup events falling along a spectrum from mechanical to thermal. Due to ongoing warming and intensification of the Arctic hydrological cycle, several studies have observed trends towards earlier ice breakup over the past 50–100 years across the pan-Arctic region (Magnuson et al., 2000; Shiklomanov & Lammers, 2014; Smith, 2000) and identified shifts towards more thermal (less severe) breakup events (Prowse, Shrestha, Bonsal, & Dibike, 2010). Available in situ observations

* Corresponding author at: Scott Polar Research Institute, University of Cambridge, Lensfield Road, Cambridge CB2 1ER, UK,

E-mail addresses: s.cooley@ucla.edu (S.W. Cooley), pavelsky@unc.edu (T.M. Pavelsky).

http://dx.doi.org/10.1016/j.rse.2016.01.004

have shown weakening ice resistance and earlier onset of spring discharge, but these data from sparsely distributed hydrologic stations may not reflect patterns of breakup within the entire river network. Without observation of river ice processes at whole river scales, it is difficult to understand how a warming climate impacts river ice breakup. Remote sensing has tremendous potential to assess large-scale patterns in breakup (Pavelsky & Smith, 2004), yet no systematic method has been developed to measure ice breakup on Arctic rivers from space.

This paper presents an automated algorithm for detecting river ice breakup continuously over the entire lengths of large northern rivers using daily time series of Moderate Resolution Imaging Spectrometer (MODIS) satellite imagery. From this surface reflectance imagery, we determine breakup dates in 10 km segments over the four largest pan-Arctic rivers, the Ob', Lena, Yenisey, and Mackenzie, from 2000 to 2014. We then analyze spatial and temporal trends in breakup timing using this dataset and examine how the spatial distribution of trends at whole river scales compares to previous point-based studies.

2. Background

2.1. River ice breakup processes: a brief review

River ice breakup events generally coincide with the annual spring flood, which is associated with increased discharge due to snowmelt. Hydroclimatic conditions during the fall and winter control the freezing level of the river, the ice thickness and the snowpack, setting the initial conditions for the breakup season (Prowse, Bonsal, Duguay, & Lacroix, 2007). The meteorological conditions during the spring melt season generally play the most dominant role in controlling breakup dynamics (Goulding, Prowse, & Beltaos, 2009). Breakup does not always progress linearly; channel geometry and confluences with other rivers also influence breakup timing. For example, the presence of thick downstream ice and favorable river morphology can lead to an ice jam and resulting heavy flooding (Beltaos, 2003).

Breakup events can be characterized as mechanical or thermal depending on the meteorological conditions governing the breakup season. Mechanical breakup events are more likely to occur when water surface elevation at freeze-up is lower, when ice is thicker, and when snowpack is larger (Beltaos, 2003). In mechanical breakup events, the rapid melting of the snowpack increases discharge levels upstream before the downstream regions have begun to melt significantly. This high flow encounters significant resistance due to thicker ice downstream, often leading to severe ice jam flooding (Beltaos & Prowse, 2009). In contrast, thermal breakup events generally occur when there is a smaller winter snowpack or delayed spring melt of snow pack, allowing downstream ice to ablate substantially before the arrival of the spring flood wave (Beltaos, 2003). The reduced strength of the downstream ice cover leads to less severe breakup events and therefore decreased flooding. Thermal events can also be characterized by a decreased surface air temperature gradient along the river (Prowse et al., 2010). Given the complexity of preexisting ice conditions and hydrometeorological forcings during the breakup season, most ice breakup events fall somewhere along this spectrum from mechanical to thermal, creating a broad range of event severity even within individual river basins (Beltaos & Prowse, 2009).

The timing of river and lake ice breakup is dependent on several climatic drivers and thus can be used to infer northern hemisphere climate variability and its impact on terrestrial systems. Numerous studies note a trend towards earlier ice breakup dates over the past 20–100 years (e.g., Magnuson et al., 2000; Prowse et al., 2007). Despite general agreement regarding a trend towards decreasing length of ice conditions, the specific mechanisms driving these changes remain unclear. Warming temperatures are hypothesized to lead to breakup through thinning of downstream ice (reduced resistance) and higher discharge (increased forcing). Numerous studies observe a strong correlation between spring air temperature and breakup timing (Bieniek et al., 2011; Goulding et al., 2009; Shiklomanov & Lammers, 2014; Smith, 2000). Winter surface air temperatures also impact breakup by influencing initial conditions within the river basin. In contrast, the effects of changing precipitation and river discharge remain uncertain. An observed earlier arrival of the spring flood (Shiklomanov, Lammers, Rawlins, Smith, & Pavelsky, 2007) may lead to earlier breakup as the timing of peak discharge is strongly correlated with breakup onset. While river discharge has increased over the past 80 years for some large northern rivers (Peterson et al., 2002), inconclusive and conflicting studies suggest that the relationship between the magnitude of discharge, precipitation and breakup timing is location dependent and poorly understood (Bieniek et al., 2011; Goulding et al., 2009; Lesack, Marsh, Hicks, & Forbes, 2014; Shiklomanov & Lammers, 2014). Natural variability and the influence of interannual, decadal and multidecadal climate oscillations such as the PDO and ENSO can also affect breakup and obscure trends (Bonsal, Prowse, Duguay, & Lacroix, 2006; Pavelsky & Smith, 2004; Prowse et al., 2007).

Though trends towards earlier ice breakup are well established, the magnitude and statistical significance of these trends vary across the Arctic region. A trend towards earlier spring breakup of 1–2 days per decade over the past 30 years has been identified in the Mackenzie River Delta (De Rham, Prowse, & Bonsal, 2008; Goulding et al., 2009; Lesack et al., 2014), but little conclusive research exists on trends in breakup timing in the central Mackenzie Basin. Studies using Russian point-based hydrologic data generally note earlier melt onset and decreasing duration of ice conditions (Ginzburg, Polyakova, & Soldatova, 1992; Shiklomanov & Lammers, 2014; Smith, 2000; Vuglinsky, 2002, 2006). In his analysis of Russian hydrologic station data, Vuglinsky (2006) identifies decreases in duration of ice conditions of 3–7 days from 1980 to 2000 for Siberian rivers. Similarly, Shiklomanov and Lammers (2014) observe decreases of between 7 and 20 days over the period 1955–2012. It is important to note that these studies all rely on the assumption that point-based breakup dates can be used to infer river-scale variability and trends.

2.2. Review of remote sensing of river and lake ice

Obtaining high spatial and temporal resolution data would substantially improve our ability to characterize river ice breakup processes. Because of the remote setting and considerable length of major Arctic rivers, most studies must rely on sparsely distributed hydrologic station data, preventing observation of spatial patterns in breakup at basin-wide scales. Furthermore, ground-based hydrologic monitoring has recently decreased across the Arctic region, limiting data available to characterize recent trends (Shiklomanov, Lammers, & Vorosmarty, 2002). Although remote sensing allows for study of river ice breakup at whole river scales, satellite imagery remains underutilized in river ice breakup research (Duguay et al., 2015; Jeffries, Morris, & Kozlenko, 2005).

Satellite imagery used for remote sensing of river ice must balance three main requirements. First, it must be possible to easily differentiate between ice, mixed ice/water and open water. Second, the imagery must be of sufficiently high spatial resolution to distinguish lakes and rivers from the surrounding landscape. Third, the temporal resolution must be sufficiently fine to allow for determination of breakup timing within a reasonable window of error. Past studies have utilized active and passive sensors in several wavelengths and from a variety of platforms to study river and lake ice. The majority of recent research on remote sensing of river and lake ice has focused on assessing the capabilities of satellite imagery or on economic applications such as locating ice jams or real-time ice detection. Only a handful of studies use remote sensing to study temporal trends in ice phenology (Latifovic & Pouliot, 2007; Pavelsky & Smith, 2004).

Due to its high spatial resolution and ability to distinguish different ice types, synthetic aperture radar (SAR) is commonly used to study river and lake ice. SAR sensors actively emit microwave radiation, allowing imagery to be collected under a wide range of lighting and atmospheric conditions. The primary benefits of SAR are its relatively high spatial resolution and insusceptibility to cloud cover. However, the low temporal resolution characteristic of most SAR sensors produces greater uncertainty in breakup date detection. Additionally, the complexity of SAR imagery can lead to some difficulty in distinguishing between ice and water, particularly when open water pools on the surface of the ice (Jeffries et al., 2005). The appearance of ice in SAR images depends on both surface and volume scattering due to factors such as the surface smoothness, dielectric constant and water content (Unterschultz, van der Sanden, & Hicks, 2009). Ice will appear bright if the surface is rough, whereas wet and smooth ice can act as a specular reflector and thus exhibit low brightness similar to open water. Because the backscatter signature depends on both the surface and the internal structure of the ice, SAR enables observation of ice properties such as the presence of water on the ice surface, ice thickness and whether the ice is frozen to the bed (Duguay et al., 2015; Mermoz et al., 2014). SAR is therefore well suited to identifying ice jams and categorizing river ice types through visual and automated classification methods (Bernier & Gauthier, 2006; Gauthier, Tremblay, Bernier, & Furgal, 2010; Sobiech & Dierking, 2013; Weber, Nixon, & Hurley, 2003).

Applications of SAR specific to river ice breakup are less common, and most studies concentrate on economic applications rather than identifying trends over significant time scales. Unterschultz et al. (2009) find that SAR can be used to determine river ice characteristics and breakup timing over a relatively short stretch of the Athabasca River. Similarly, Floyd, Prakash, Meyer, Gens, and Liljedahl (2014) examine a time series analysis of SAR images over the Kuparuk River in Alaska, observing that variance in brightness is the most reliable indicator of breakup onset. In the future, given the increased temporal resolution and availability of SAR images from satellites such as ScanSAR and Sentinel-1, SAR images may enable reductions in cloud uncertainty in ice breakup detection as compared to optical imagery. A few studies have also explored the applicability of synthetic aperture radar interferometry (InSAR) to ice breakup research, finding that InSAR can be used to detect river ice motion and predict locations of mechanical breakup (Smith, 2002; Vincent, Degroeve, Edwards, & Abolfazl Mostafavi, 2004).

Optical satellite sensors commonly provide imagery of snow and ice at global scales and are thus useful for detection of river and lake ice. High-resolution images from satellites such as Landsat (30 m) can be used to map ice extent on rivers and lakes (Gatto, 1990; Sakai et al., 2015) and can provide a helpful baseline reference in SAR research (Cook & Bradley, 2010; Nolan et al., 2002). However, the low temporal resolution and small areal extent of Landsat scenes reduce their utility for large-scale breakup research. Optical imagery at moderate spatial resolution (0.25–1 km) and high temporal resolution from sensors such as the Advanced Very High Resolution Radiometer (AVHRR) and the Moderate Resolution Imaging Spectrometer (MODIS) has several advantages for study of ice breakup. Ice is easily distinguishable from water in near-infrared bands, and the daily coverage allows for high temporal precision. The coarser resolution restricts their use to major rivers and lakes, however, and cloud-obscured imagery limits temporal accuracy, particularly in the cloudy sub-Arctic region. Early research using moderate resolution optical imagery generally has involved visual interpretation of VHRR and AVHRR data to determine river and lake ice breakup timing over a few breakup seasons (Dey, Moore, & Gregory, 1977; Maslanik & Barry, 1987; Wynne & Lillesand, 1993).

More recent studies use time series of MODIS/AVHRR to examine river and lake ice phenology. Pavelsky and Smith (2004) determine the date of ice breakup at basin scales for four large northern rivers through visual examination of MODIS and AVHRR satellite imagery. Their results demonstrate that MODIS imagery is valuable in examining breakup at large scales, and they find breakup dates determined from remote sensing to be highly correlated to Russian hydrologic station data. Latifovic and Pouliot (2007) develop a method that detects breakup and freeze-up using time series of surface reflectance and brightness values from AVHRR data for 42 Canadian lakes, also noting a strong correlation between AVHRR analysis and in situ data. Similarly, Kropáček, Chen, Hoerz, and Hochschild (2013) examine patterns in ice phenology of lakes on the Tibetan Plateau using MODIS 8-day composite imagery. Other studies focus on real-time ice detection and economic applications for industrial areas. Chaouch et al. (2014) present an automated method of mapping ice extent using MODIS data on the Susquehanna River in Pennsylvania primarily for real time ice detection purposes. While some employ a similar approach to the method described in this paper, these studies do not develop a breakup detection method intended for identification of spatial and temporal trends in breakup timing (Chaouch et al., 2014).

3. Study area

We examine the four largest rivers draining into the Arctic Ocean: The Mackenzie in northwest Canada, and the Yenisey, Ob' and Lena in Siberia (Fig. 1). These four rivers have a significant impact on the Arctic ocean freshwater budget (Serreze et al., 2006) and are generally ice-covered for six months of the year or more (Bennett & Prowse, 2010). Discharge and corresponding freshwater input to the Arctic ocean are increasing for all four rivers as part of the intensifying hydrological cycle and rapid climate changes occurring in the Arctic region (Déry, Hernández-Henríquez, Burford, & Wood, 2009; Peterson et al., 2002). Several studies have examined breakup patterns in these rivers using point-based station data, remote sensing or a combination of methods (e.g., de Rham et al., 2008; Lesack et al., 2014; Pavelsky & Smith, 2004; Shiklomanov & Lammers, 2014), which allow us to compare our results with prior efforts. Our ability to accurately assess breakup timing depends chiefly on the width of the river examined. Breakup detection is most reliable for rivers wider than ~500 m. We determine breakup dates over the entire Mackenzie (1580 km) and for the Yenisey starting at the confluence with the Angara (1880 km) since they are always sufficiently wide over these reaches. We focus on the lowermost 2800 and 2460 km of the Lena and Ob', respectively, where the rivers are greater than ~500 m wide and the state of their ice cover is distinguishable using 250 m MODIS imagery. We examine breakup timing for 2000–2014, the full extent of the MODIS record.

4. Methods

4.1. Datasets

We use daily MODIS composite imagery (MOD09GQ, collection 5) for this analysis due to its high temporal resolution and adequate spatial resolution. The principal advantage of MODIS is its daily availability, allowing for breakup detection at high temporal resolution. We use band 2 surface reflectance (841–876 nm) because it is available at 250 m spatial resolution and because it is comparatively simple to distinguish among ice, mixed ice/water and open water in the near infrared. The 250 m resolution is sufficient for breakup detection on rivers wider than 500 m, making it suitable for the large-scale analysis of major rivers presented here. MOD09GQ is a daily composite product that selects the best available data on a pixel-by-pixel data, resulting in very low incidence of missing or poor-quality data (Vermote, Kotchenova, & Ray, 2011). Other MODIS bands and derived products may be potentially useful in some aspects of river ice detection, but including more bands did not substantially improve our results and thus did not outweigh the decreased algorithmic efficiency. For cloud detection, we use MOD35_L2, the MODIS cloud mask product, gridded to 1 km resolution (Ackerman et al., 2010).

Comparison with ground observations of breakup enables validation of our breakup detection approach. We use Water Survey of Canada (WSC) hydrometric records for the Mackenzie and Russian ice phenology records for the three Siberian rivers (Shiklomanov & Lammers, 2014) to compare the satellite breakup dates determined from the

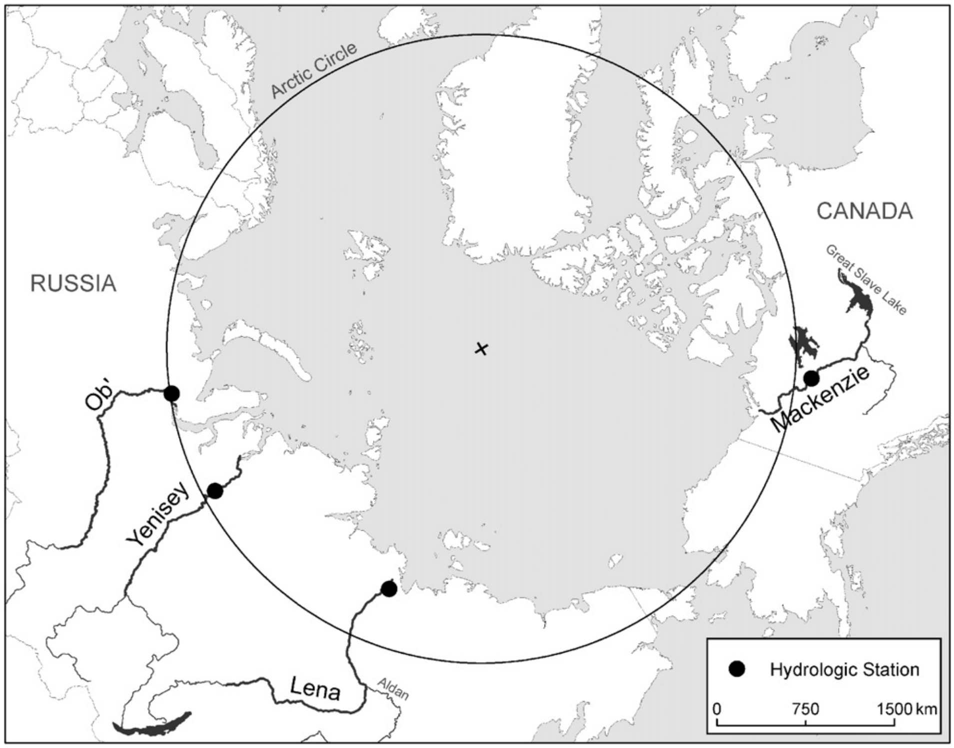

Fig. 1. Locations of the four rivers studied. The river extent sufficiently wide for analysis using MODIS imagery is shown in black.

algorithm to ground data. WSC hydrometric data includes the 'Last B Date', the last day where ice conditions are assumed to impact the river's flow in the vicinity of the station (de Rham et al., 2008). It is important to note that WSC stations do not record visual observations of actual breakup dates of the river; rather the 'Last B Date' is generally an estimate from available data. The Russian data includes the conclusion date of ice events, considered to be the date of ice disappearance (Smith, 2000). Since the timing of the peak flood is commonly highly correlated with the timing of ice breakup, we also examine discharge data. For the Mackenzie, the date of peak discharge is determined using WSC discharge records. For the Siberian rivers, discharge data is available from ArcticRIMS, a data repository at the University of New Hampshire (Shiklomanov & Lammers, 2014). We do not examine discharge data for the Ob', as the timing of peak discharge is ordinarily considerably after breakup due to the extensive impact of regulation at upstream dams.

4.2. Ice breakup detection algorithm

We detect breakup dates for each river using the following automated method:

1. We download daily MODIS band 2 surface reflectance imagery and cloud mask over the entire breakup season (approximately April 1st to July 1st) for each river from 2000 to 2014.
2. We identify five cloud-free ice-covered images and five open water images from a range of years for each river. We average the five ice-covered and five open water images and compute the normalized difference in band 2 reflectance between the ice and water averages. We define river extent as all areas exhibiting both ice cover and open water states, practically defined as pixels with a normalized difference >0.75, as we find this tolerance sufficiently demarcates river area. We then use this difference to create a binary river extent mask and then manually correct this river mask to remove all non-river water pixels.
3. We use an existing high resolution river centerline for the Mackenzie (Allen & Pavelsky, 2015) and manually digitize centerlines for the Siberian rivers. From this centerline, we split the river into segments approximately 10 km in length. We then match each river mask pixel to the nearest centerline pixel, yielding river mask segments equal in length (~10 km) but not necessarily equal in river surface area.
4. For each daily image, we classify each river pixel as snow/ice (band 2 reflectance >0.5), mixed ice/water (0.1–0.5) or open water (<0.1). The thresholds used for these classifications were determined through a frequency analysis of river pixel values for days when the river is known to be ice-covered or open water (Fig. 2). This classification is performed over every scene for the entire breakup season.
5. Using the MOD35_L2 Cloud Mask, we determine the number of cloudy and clear pixels in each river segment for each day of the breakup season. If more than 50% of the pixels in any river segment are flagged as cloudy, the river segment is classified as cloudy.
6. We use the daily classified river images and the cloud mask to determine how the river surface changes over the breakup season. For each non-cloudy river segment, we sum the total number of pixels classified as water. We then determine the first day for which 75% of the pixels in the river segment are classified as open water, which we define as the detected date of breakup. We use 75% water as the breakup threshold because it distinguishes the first day where the river reach is predominantly open water while allowing for some classification error associated with temporal variability in river extent and location. We find increasing the breakup threshold leads to missed breakup detection due to variations in inundation extent and minor errors in the river mask, especially in narrow or braided sections.
7. Using the cloud mask, we determine the number of days prior to the date of breakup where the river segment was cloud-obscured, meaning the algorithm could not detect breakup. If there is more than one cloudy day before the date of breakup, we consider the corrected date of breakup to be the midpoint of the cloudy period (Pavelsky & Smith, 2004). The window of uncertainty around each breakup date is then the number of days between this midpoint and the detected date of breakup.

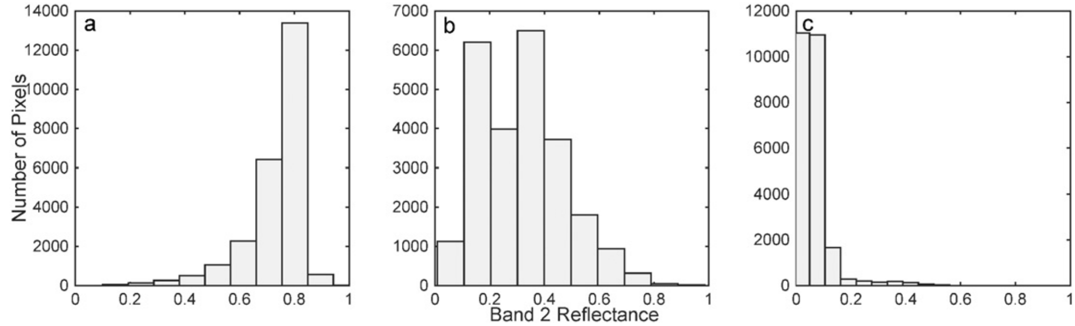

Fig. 2. Histograms of band 2 reflectance values for three 100 km segments of the lower Lena in 2013, the lower Yenisey in 2009 and the middle of the Lena in 2005 during a) pre-breakup, (days 120, 130 and 121, snow and ice-covered), b) mid-breakup (days 152, 145 and 143, mixed ice/water) and c) post-breakup (days 153, 158 and 147, open water). There is not a statistically significant difference in the water/ice contrast among the four rivers examined.

4.3. Error analysis

The first component of error estimation in our method is the accuracy of the classification of ice/no-ice. Error resulting from poor quality MODIS imagery is inconsequential; analysis of MODIS quality flags shows that >99% of river pixels are quality data. An analysis of view angle variation in ice-covered and open water images also demonstrates that there is no correlation between view angle variation and band 2 reflectance in ice and open-water pixels. Additionally, all images were manually checked for data collection errors. The radiometric contrast between mature ice cover and open water in optical imagery (e.g., MODIS) is widely recognized as very robust (Hall, Riggs, & Barton, 2001). However, without large-scale ground observations of river conditions, which do not exist, it is not possible to directly ground truth our assessments of ice/water contrast. Instead, we use visual examination of imagery, sensitivity analyses, and comparison with existing ground breakup data to check the ice/no-ice classification process. Additionally, as our breakup detection method relies on the aggregate classification of many pixels over 10 km reaches, errors caused by factors such as cloud shadows and water on top of ice, which may affect a few pixels at a time, are likely to be minimized. Overall, sources of error derived from the ice/no-ice classification are likely to be substantially smaller than those caused by cloud-obscured imagery.

By far the largest source of error in estimation of breakup dates is cloud-obscured imagery, a common problem in optical remote sensing. Using the MODIS Cloud Mask product, we employ a 50% cloud tolerance to ensure that we are able to obtain accurate river surface reflectance data for each segment classified as clear. The relatively coarse resolution (1 km) of the MODIS cloud detection methodology as compared to the surface area of each 10 km river segment (between 5 and 40 km^2) means changing the algorithm's percent cloud tolerance has little impact on the number of segments classified as cloudy.

Another smaller source of error derives from the river masks used to distinguish between land and water pixels. For simplicity and consistency, we build the binary river masks from MODIS reflectance imagery using the difference in surface reflectance values between ice-covered and open water imagery, averaged over five different years. The location and extent of the four rivers studied here generally do not vary significantly from year to year. The only exceptions occur in an especially flat and braided reach of the Ob', where changing inundation levels can affect the river's location and extent. Substantial year-to-year deviations from the mean river location can result in missed breakup detection. Rather than recalculating the river mask for each year and compromising the consistency of segment boundaries, we removed from consideration several segments of the Ob' where the river migrates substantially. The number of segments removed is small, averaging fewer than 1 segment removed per 100 km, and does not substantially impact the overall results.

4.4. Data smoothing

We use 10 km river segments for breakup detection because the short length allows for examination of relatively small-scale breakup processes. Shorter segments and therefore fewer pixels per segment increase error due to variability in river extent and location, particularly in narrow or braided segments. Breakup dates exhibit substantial noise when detected over 10 km reaches (Fig. 3). Though some of this variability is a natural signal caused by confluences with other rivers and mechanical breakup events, much of it is likely caused by cloud-obscured imagery. Sensitivity analyses involving testing 25% and 75% for the cloud threshold also indicate that the cloud tolerance has little impact on this variability. To reduce the impact of cloud error, we smooth the breakup dates using a 10-point (100 km) moving average filter (Fig. 3). Application of this filter maintains large-scale natural signals and highlights spatial and temporal patterns in breakup timing.

4.5. Trend and correlation calculation

To determine trends in breakup timing over the 15-year period, we use the nonparametric Mann-Kendall test (Helsel & Hirsch, 1992), which is commonly used in similar hydrological studies (e.g., Goulding et al., 2009; Lesack et al., 2014; Shiklomanov & Lammers, 2014; Smith, 2000). A least squares linear regression is then applied to the 15-year time series for each 10 km segment and to whole river averages of

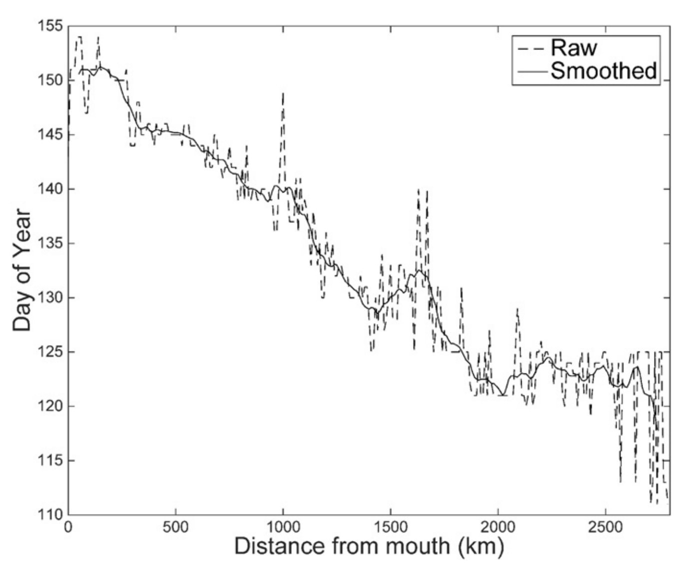

Fig. 3. Raw breakup dates (dashed) and smoothed breakup dates using a 10-point moving average filter (solid) for the Lena in 2014, plotted by distance from mouth (km).

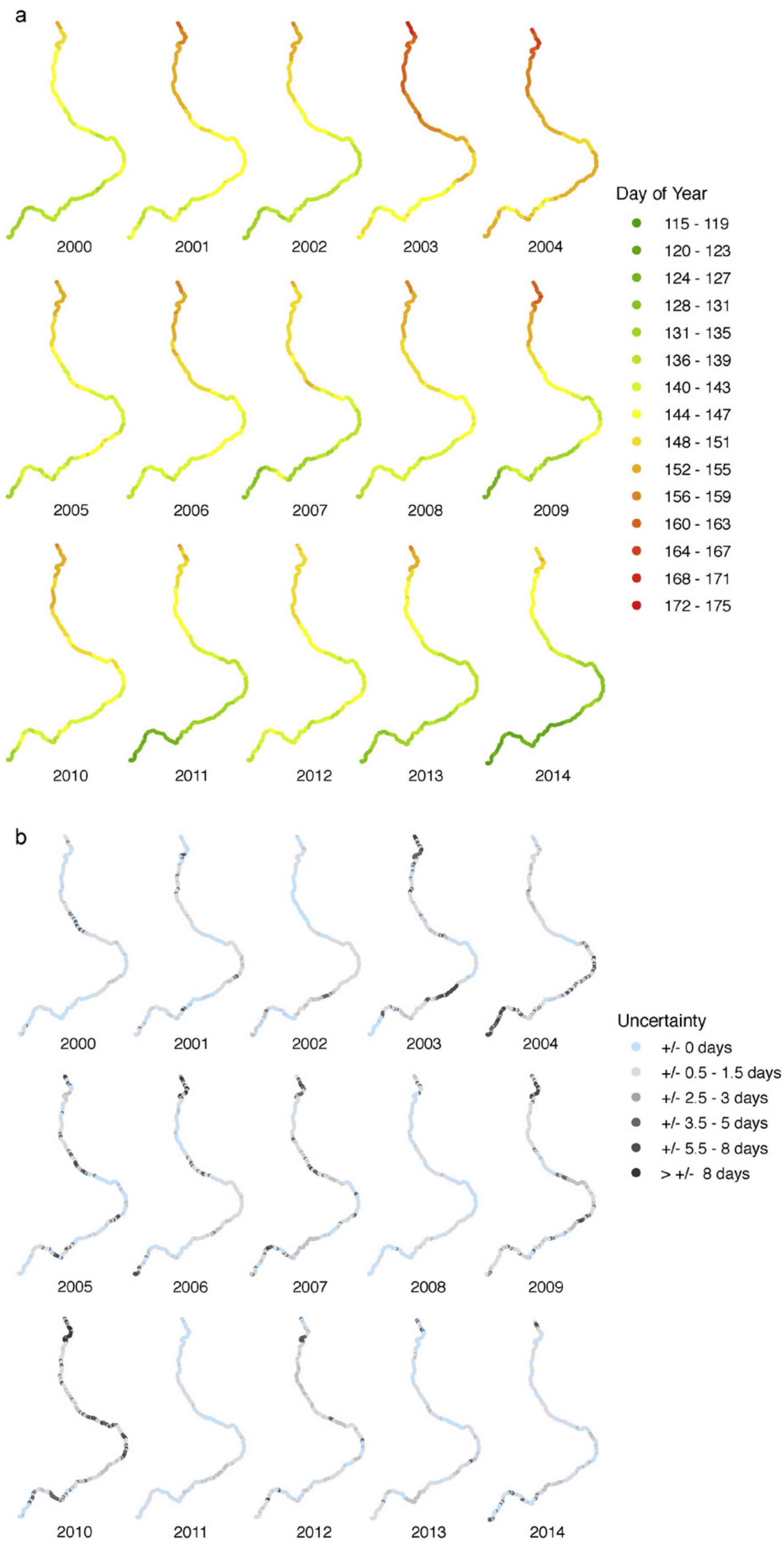

Fig. 4. Breakup dates (a) and uncertainty due to cloud-obscured imagery (b) for the Lena from 2000 to 2014. River reach shown is approximately 2800 km.; location is shown in Fig. 1.

breakup timing. We consider trends to be statistically significant at the 90% level. For assessing correlations between time series of breakup date on different rivers and examining relationships between upstream and downstream breakup timing, we use Pearson's correlation coefficient.

5. Results

5.1. Spatial patterns in breakup

Using the method described in Section 4, we determine dates of breakup for all four study rivers during the period 2000–2014. We show breakup dates and uncertainty associated with cloud contamination on the Lena for each year to illustrate large-scale breakup patterns and the variability in cloud uncertainty (Fig. 4). We find a mean breakup window of ± 1.3 days, with significant variability among rivers and years. Due to differing climatic conditions governing western Canada versus central and eastern Siberia, the percent of river segments classified as clear (cloud <50%) varies among the four rivers, ranging from 40.2% for the Yenisey to 50.8% for the Mackenzie (Table 1). The average window of uncertainty for each breakup date also varies by river and by year (Table 1). Despite the significant amount of cloud-obscured imagery, for all four rivers examined, we are able to detect breakup within a window of ± 1 day for the majority of river segments.

By plotting dates by distance from mouth, we are able to discern spatial patterns in breakup (Fig. 5). For each river, breakup primarily progresses monotonically northward and downstream. There is considerable variability from year to year in the timing and length of breakup, but the overall spatial patterns remain similar. All four rivers show evidence of discontinuous breakup, where a section may breakup several days or more after the surrounding river segments. These later breakup events are generally caused by tributaries and channel morphology; however, due to natural variability these events are not always consistent from year to year.

Distinct patterns characteristic of each river emerge upon closer examination of the data. On the Mackenzie, breakup first occurs at the confluence with the Liard River, 300 km downstream from the initiation of the Mackenzie at Great Slave Lake. This pattern is likely due to warmer surface air temperatures in the Liard River basin and the influence of Great Slave Lake, which attenuates the impact of any flood wave generated by upstream melt and generally remains ice-covered until after the main stem of the Mackenzie has broken up. We observe significant spatial and temporal variability in the upstream portions of the Lena and relatively smooth progression of breakup downstream. The transition into more temporally consistent breakup occurs near the confluence of the Lena and the Aldan rivers, 1260 km from the mouth, suggesting that the addition of the Aldan moderates variability in breakup timing in the lower Lena. On the Ob', the northward and downstream progression of breakup reverses slightly between approximately 1300 and 900 km from the mouth. This section of the river is associated with a change in the direction of the along-river temperature gradient (Prowse et al., 2010). As the river moves westward towards European Russia, the surface air temperatures actually increase downstream until the river again turns northward and eastward, likely explaining the observed reversal in breakup timing.

Table 1
Total percent clear segments and mean breakup window due to cloud-obscured imagery for each river.

River	Percent clear segments	Mean breakup window ($\pm$ days)
Mackenzie	50.83	0.91
Lena	42.78	1.33
Ob'	40.78	1.24
Yenisey	40.20	1.62

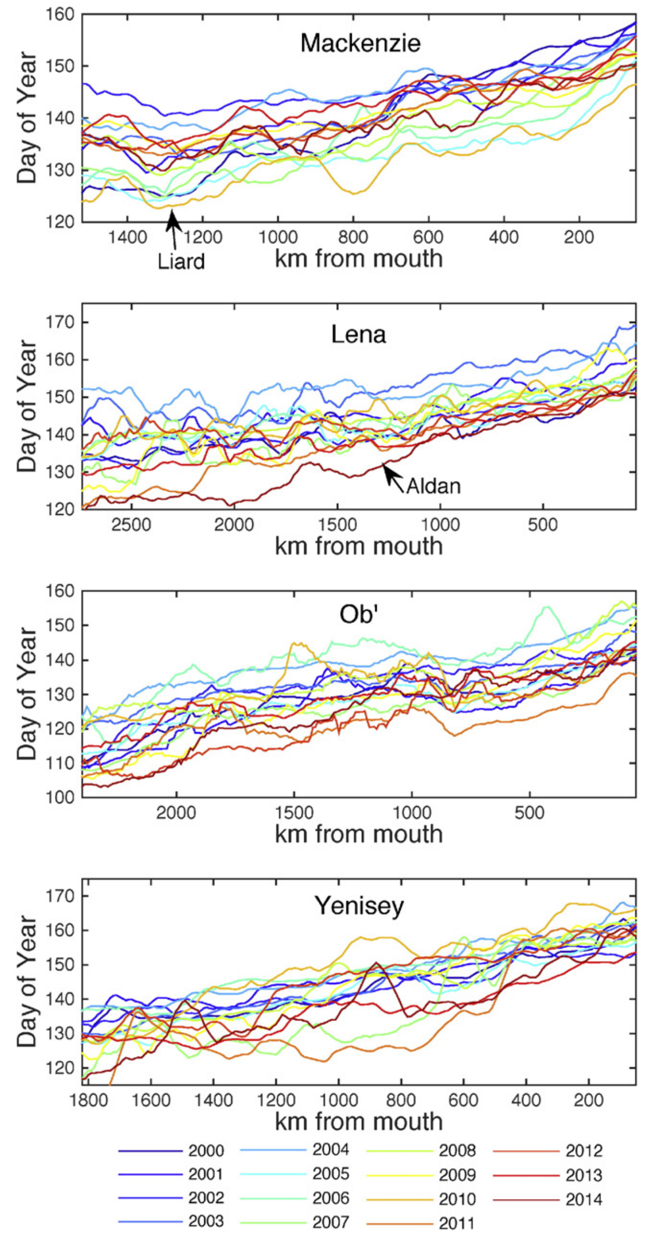

Fig. 5. Breakup dates plotted by kilometers from the mouth. Locations of major tributaries are noted for the Lena and Mackenzie.

The mean date and length of breakup vary significantly among rivers and from year to year. While ice breakup does not progress downstream monotonically, breakup generally advances more rapidly on the Lena and the Ob', the longer, more braided rivers, at average rates of 79.8 km/day and 57.2 km/day respectively. On the shorter and straighter Yenisey and Mackenzie rivers, breakup moves at average rates of 50.5 km/day and 41.7 km/day respectively. The range of breakup rates observed also varies significantly by river and by year, with a maximum rate of 100 km/day on the Lena (in 2000, 2001 and 2012) and minimum of 37.1 km/day on the Mackenzie (in 2000).

5.2. Comparison with ground data

Breakup dates calculated here are highly correlated with ground observations of ice breakup (Fig. 6) for the Mackenzie, Lena and Ob' rivers. There is not a strong correlation between the detected dates and ground data for the Yenisey; however, the ground breakup dates for the Yenisey over the period 2000–2012 are extremely variable, and our results

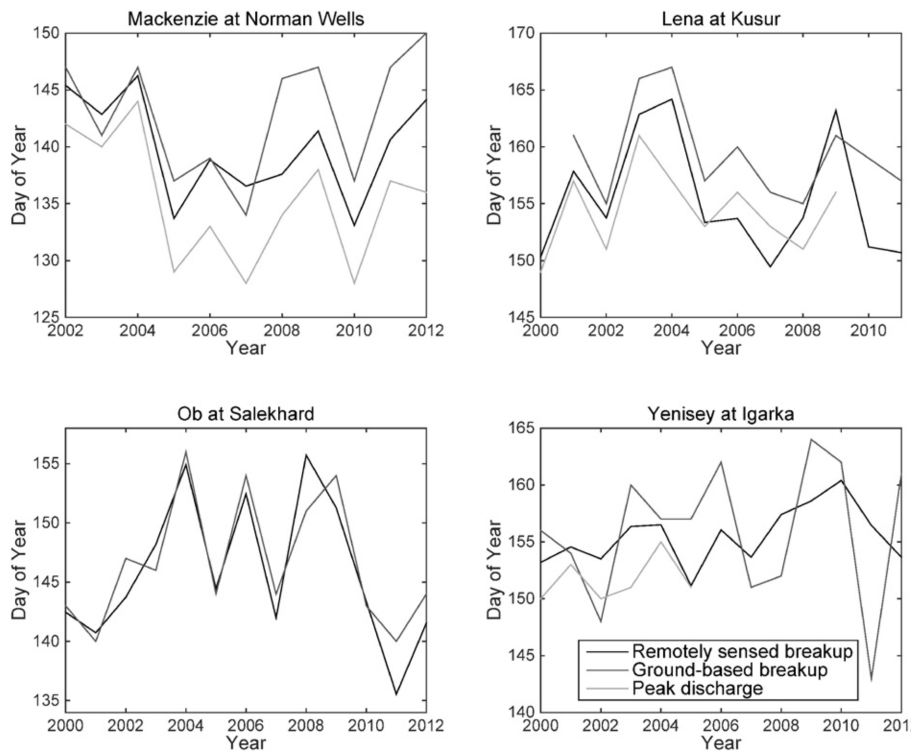

Fig. 6. Comparison of remotely sensed breakup date, ground breakup date and timing of peak discharge for the Mackenzie at Norman Wells, the Lena at Kusur, the Ob at Salekhard and the Yenisey at Igarka.

suggest that they may not be accurate. Additionally, though available discharge data only overlaps with the MODIS time series from 2000 to 2005, remotely sensed breakup dates on the Yenisey are correlated with the timing of peak discharge. A strong correlation between breakup timing and peak discharge is also found on the Lena and Mackenzie. The strong correlations between remotely sensed breakup, ground observations of breakup and the timing of peak discharge are consistent with scientific understanding of river ice processes and suggest that the algorithm presented here accurately measures breakup timing.

5.3. Temporal patterns in breakup

To examine how breakup patterns are changing, we calculate trends in breakup timing over the past 15 years for all 10 km segments of each river. Where trends are statistically significant, they are universally negative and range between -0.25 and -1.25 days per year. However, the magnitude and statistical significance of the trends vary considerably along each river (Fig. 7). For the Lena, we find statistically significant trends across the majority of the river, with the magnitude of the trends highest in upstream reaches. The Mackenzie displays a strong trend towards earlier breakup near the delta but no statistically significant trend for the middle and upstream reaches. Trends on the Yenisey and the Ob' also only occur in distinct sections; strong trends are found in the upper Yenisey and the middle to upper Ob'.

When examining whole river averages, we find breakup timing to be correlated between the three Siberian rivers (mean $r = 0.68$) but observe no significant correlation between the Russian rivers and the Mackenzie (Fig. 8a). Only the Lena has a statistically significant trend towards earlier breakup averaged over the whole river. We also examine patterns in the timing of breakup initiation, the end of breakup and the length of breakup (Fig. 8b–d). There is a statistically significant trend indicating earlier initiation of breakup for the Lena, whereas for the Mackenzie we find trends towards earlier breakup completion and decreasing breakup length. Despite clear trends towards earlier breakup in the middle and upper sections of the rivers, trends in mean breakup date for the Ob' and Yenisey rivers are not statistically significant.

To better understand the controls on breakup timing, we examine statistical relationships among different measures of breakup timing. We correlate mean breakup date and total breakup length with each other and with the first and last dates of breakup and the mean date of breakup for the uppermost and lowermost quarters of the river (Table 2). In general, upstream processes seem to be strongly related to overall breakup timing. On the Lena, Mackenzie and Yenisey, the timing of breakup initiation and the mean breakup date in the uppermost river section are more strongly correlated to both the whole-river mean breakup date and the breakup length. Upstream and downstream breakup are equally correlated to overall breakup timing on the Ob'.

6. Discussion

6.1. Monitoring ice breakup

The results described here indicate that it is possible to accurately detect river ice breakup dates from MODIS imagery with low uncertainty (±1.3 days, on average). The first notable advantage of this approach over other methods of monitoring ice breakup is the ability to determine whole-river spatial patterns in breakup timing. Ground-based research is inherently limited by the remoteness and inaccessibility of these major Arctic rivers, especially during the breakup season, and must thus rely on point-based data collected at widely dispersed locations. Considering the current interest in understanding how climate warming and the intensification of the Arctic hydrologic cycle impact river ice breakup, several studies cite a need for improved research on whole river processes (e.g., Beltaos & Prowse, 2009). The continuous along-river breakup dates determined through this method enable simultaneous examination of temporal trends and spatial variability, which is essential to improved understanding of breakup mechanisms.

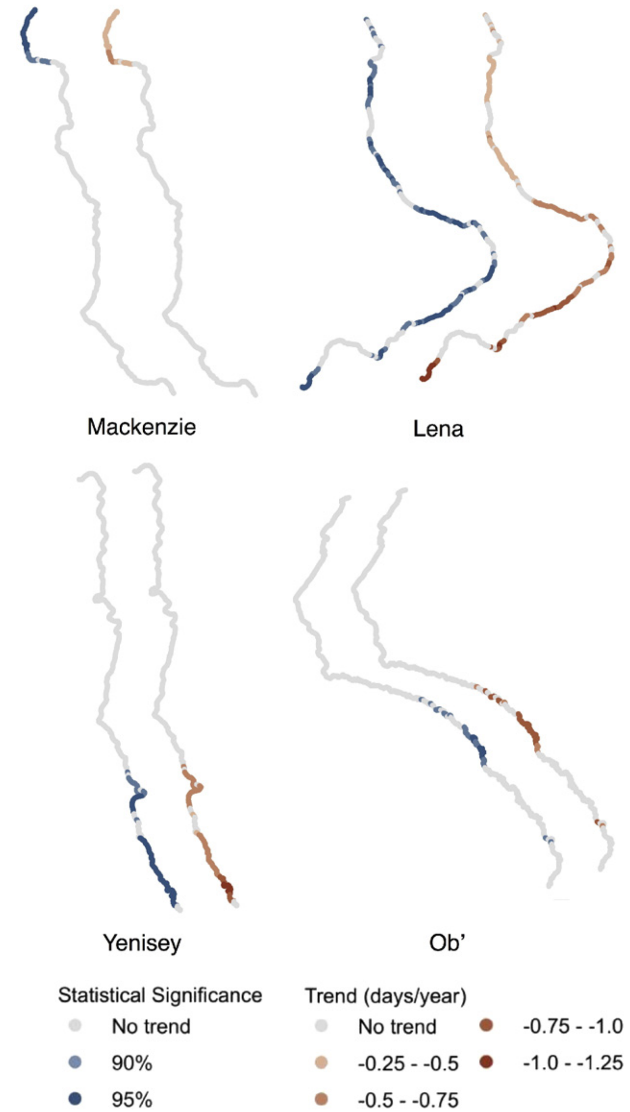

Fig. 7. Trends in breakup timing in individual river segments from 2000 to 2014. Statistical significance determined from the Mann–Kendall test is in blue on left, magnitude of trend in red on right.

Another significant advantage of the method presented here is the consistency in breakup detection. Comparison of trends in river ice phenology between rivers using ground-based data is challenging because hydrologic stations often use different definitions of critical river-ice characteristics (e.g. Catchpole & Moodie, 1974). In their study of breakup timing using station data in the Mackenzie River Basin, de Rham et al. (2008) choose to primarily use breakup indices determined from hydrographs, finding that the last 'B' dates (end of ice conditions) are not sufficiently reliable for their basin-scale analysis. Additionally, most previous studies using optical satellite imagery rely on visual examination, meaning their breakup dates are dependent on manual interpretation of imagery (e.g., Pavelsky & Smith, 2004). The method described in this paper uses one standard breakup metric, defining breakup in each 10 km segment as the first date when 75% of river pixels are open water. This consistency allows for trend analysis and comparison not only within individual river basins but also across the entire Arctic region. Considering the current decline in Arctic river observations (Shiklomanov et al., 2002), new methods like the one presented here are essential to detection and analysis of Arctic environmental change in response to warming temperatures.

As with many optical remote sensing studies, a significant disadvantage of this method is that rivers are often cloud-obscured. While cloud-obscured imagery limits the accuracy to an average window of approximately $\pm$1.3 days, the temporal accuracy remains high because MODIS imagery is available daily. Unfortunately, this high temporal resolution is counterbalanced by a relatively coarse spatial resolution (250 m), so it is not possible to distinguish very small-scale breakup processes. Breakup detection using this method is generally not suggested for segments of less than 10 km except on the widest river reaches. Additionally, the algorithm is only practical for examination of rivers wider than ~500 m.

6.2. Spatiotemporal trends in breakup timing

The temporal trends observed in this analysis, where statistically significant, consistently reflect a shift towards earlier breakup timing. The general agreement in direction of trends suggests that at large scales, point-based trend analyses (e.g. Magnuson et al., 2000) can be used to infer regional climate variability. However, the considerable variability in the magnitude and significance of trends along each river indicates that point-based trends do not necessarily reflect spatial patterns in breakup and the processes that drive them.

While Arctic warming is expected to cause earlier breakup, the net impact of warming temperatures on spatial patterns in river ice breakup for northward-flowing rivers is very complicated and difficult to predict. Despite this complexity, two hypotheses have emerged regarding the future of ice breakup processes in the Arctic. In the first hypothesis, warmer spring temperatures would lead to a decrease in the mechanical strength of the ice cover and thus weaker resistance downstream. Combined with a thinner ice cover at the start of the breakup season caused by warmer winter temperatures, we would expect to observe a shift towards breakup events controlled by weakening downstream resistance, perhaps leading to more thermal breakup events (Prowse et al., 2007, 2010). In the second hypothesis, projected increases in both surface air temperature and precipitation at northern latitudes due to an intensifying Arctic hydrological cycle (Brown & Mote, 2009; Déry et al., 2009; Rawlins et al., 2010) would lead to earlier onset of spring discharge increases upstream (Shiklomanov et al., 2007). Additionally, earlier occurrences of breakup, at a time of year with lower amounts of shortwave radiation, would limit reductions in downstream resistance due to the dependence of ice strength on internal melting and shortwave radiation absorption (Hicks, Cui, & Ashton, 2008). Consequently, an earlier arrival of the driving force could increasingly govern breakup processes. While simplifications of complex ideas, we will consider these two different hypotheses for changing whole-river scale breakup processes due to warming temperatures as either resistance/downstream-driven (decreasing ice strength) or forcing/upstream-driven (earlier onset of peak discharge).

The spatial analysis of temporal trends presented here can provide some insight into possible changes in breakup processes represented by these two hypotheses. On the Mackenzie, we detect a strong trend in the downstream reach of the river with no corresponding trend in the majority of the river. Several previous studies have found similar statistically significant trends in the Mackenzie River Delta region (de Rham et al., 2008; Goulding et al., 2009; Lesack et al., 2014). Lesack et al. (2014) attribute the earlier breakup trend in the delta to reductions in ice strength during the breakup season caused by local spring warming, finding no correlation between peak discharge levels and breakup timing. Considering the preferential warming of the downstream region, the absence of a trend in the main stem of the Mackenzie is consistent with their conclusions that a decreasing resisting force is a primary driver of the trend towards earlier breakup in the delta. Additionally, we identify a corresponding decreasing trend in the length of the breakup season on the Mackenzie, suggesting that the warming temperatures in the delta are leading to a shorter breakup season caused by weakening downstream resistance. This observation

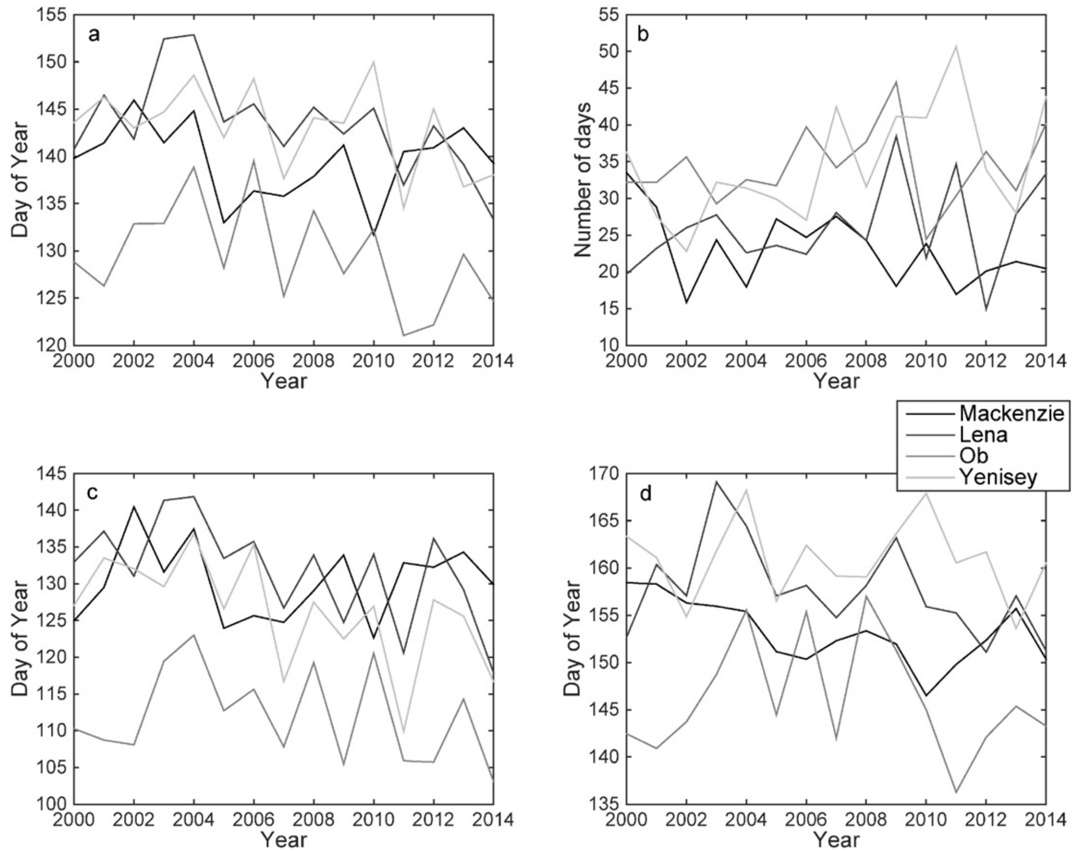

Fig. 8. Time series of mean breakup date (a), length of breakup (b), earliest date of breakup (c) and final date of breakup (d) for each river from 2000 to 2014.

supports the idea that identifiable shifts in breakup timing are largely due to decreasing resistance-driven forces.

The patterns observed for the Siberian rivers are somewhat more complex and less conclusive. In general, there exists significantly less research on breakup timing on the Siberian rivers, and nearly all recent studies rely on point-based measurements from a single station near the mouth of each river (e.g. Shiklomanov & Lammers, 2014; Smith, 2000; Vuglinsky, 2006). As a result, it is more difficult to understand how the observed spatial patterns compare to previous studies. In contrast to the Mackenzie, the magnitude of trends generally increases upstream on the Lena and the Yenisey (Fig. 7), and we observe earlier initiation of the breakup season. However, the earlier beginning of breakup is not coupled to a statistically significant trend in the length of the breakup season. The trends identified do not support predictions that the largest changes in river ice processes will be found closer to the mouth due to weakening ice strength and a decreasing downstream temperature gradient (Prowse et al., 2010). Considering the evidence that the initiation of breakup dominantly impacts the mean timing and length of breakup on the Lena and Yenisey (Table 2), these results suggest that development of a flood wave from upstream snowmelt is the principal driver of breakup processes. Since breakup initiation is related to the onset of the spring freshet from a melting snowpack, upstream-driven breakup implies that a warming climate leads to earlier breakup through earlier onset of elevated spring discharge.

On the Ob', a statistically significant trend towards earlier breakup is found where the river shifts towards westward flow (Fig. 7). This river reach corresponds to the beginning of the temperature gradient reversal on the Ob', a reversal also evident in the spatial pattern of breakup progression. The trend towards earlier breakup found solely in this portion of the river suggests that possible changes in this gradient are impacting breakup processes. The anomalous correlations between upstream processes and mean breakup timing for the Ob' are perhaps also due to the effects of the temperature gradient reversal. However, a more complete understanding of the observed patterns would require additional analysis involving along-river temperature data.

Spatial patterns of breakup trends on the three Siberian rivers point towards the second of the two hypotheses: a shift towards discharge-driven breakup. Increasing precipitation (e.g., Rawlins et al., 2010) and discharge (e.g., Peterson et al., 2002) are both significant components of the intensifying Arctic hydrological cycle. Substantial evidence demonstrates that this rising precipitation and discharge are not coupled to increased magnitude of peak discharge but rather to earlier onset of peak discharge and increased base flow (Shiklomanov et al., 2007; Smith, Pavelsky, MacDonald, Shiklomanov, & Lammers, 2007). Our results are consistent with these observations and suggest that earlier breakup is driven by earlier onset of peak discharge combined with prolonged melt, pointing towards a longer breakup season and more severe mechanical breakup events. For the Mackenzie, these relationships

Table 2
Correlations between mean breakup date and breakup length and the first and last days of breakup and the mean breakup date in the uppermost and lowermost quarters of the river.

	Mackenzie		Lena	
	Mean breakup date	Breakup length	Mean breakup date	Breakup length
Mean breakup date		−0.50		−0.41
Earliest breakup date	0.91	−0.78	0.91	−0.72
Last breakup date	0.67	0.27	0.77	0.22
Mean breakup in upper fourth	0.90	−0.76	0.96	−0.62
Mean breakup in lower fourth	0.81	0.06	0.88	0.03
	Ob'		Yenisey	
	Mean breakup date	Breakup length	Mean breakup date	Breakup length
Mean breakup date		−0.01		−0.44
Earliest breakup date	0.80	−0.47	0.81	−0.85
Last breakup date	0.83	0.37	0.63	0.34
Mean breakup in upper fourth	0.91	−0.36	0.81	−0.73
Mean breakup in lower fourth	0.87	0.43	0.60	0.37
Statistical Significance				
	99%	95%	90%	

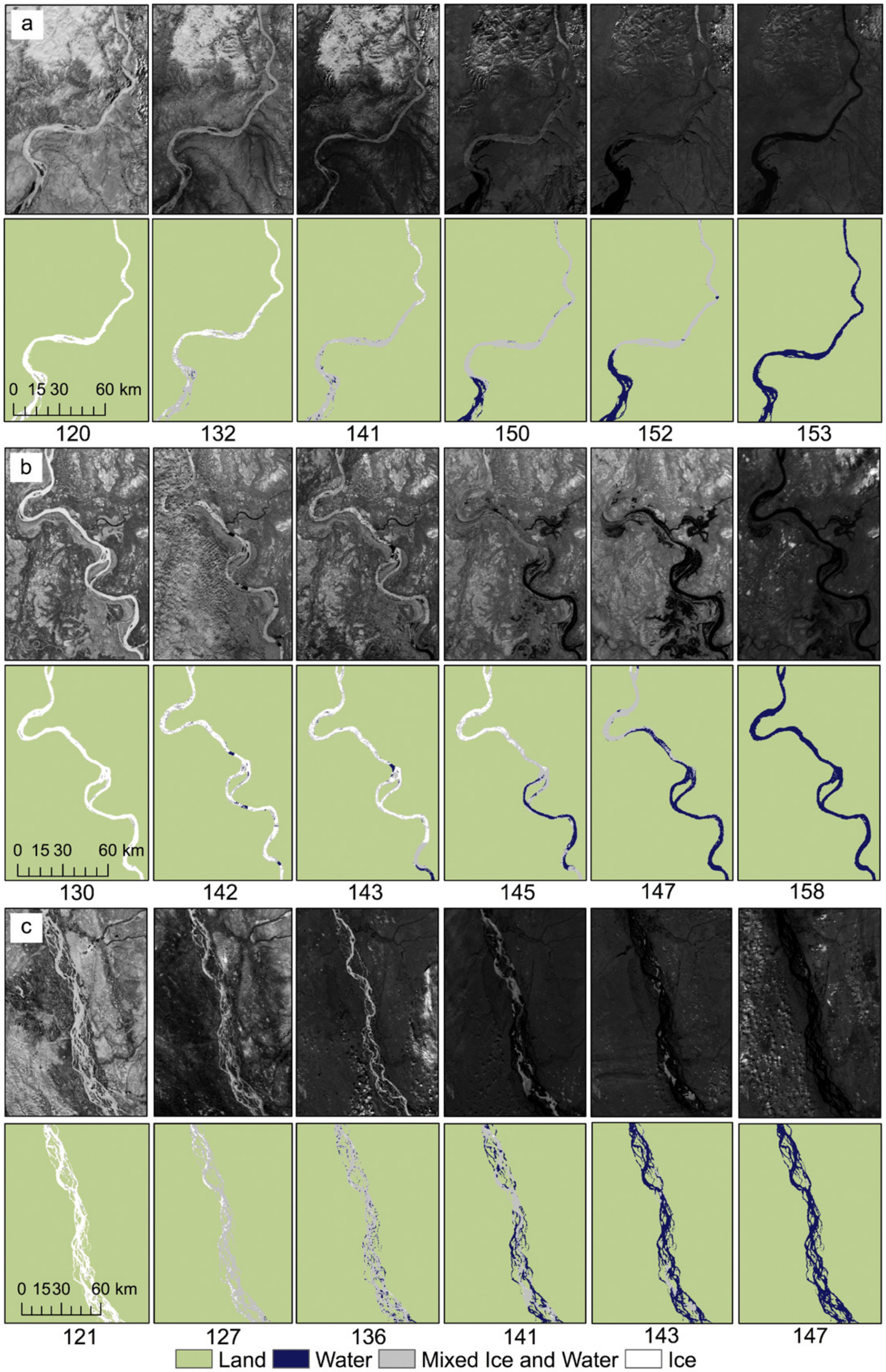

Fig. 9. Time series of a hypothesized thermal breakup event (a) on the Lena in 2013, a mechanical breakup event (b) on the Yenisey in 2009 and a morphologically constrained breakup event (c) on the Lena in 2009. The top rows show the original MODIS band 2 imagery and the bottom rows illustrate the algorithm's classification of the image. Green is land, blue is water, gray is mixed ice/water and white is snow/ice.

are perhaps more complex. The trend towards a shorter breakup season is consistent with a decreasing temperature gradient and a weaker resisting force, yet we still observe upstream breakup timing exerting a more powerful control on overall breakup timing.

Without corresponding along-river discharge and temperature data, these conclusions remain speculative. Given the complexity of the various factors impacting breakup, the observed patterns are likely the result of a combination of processes. Considering also the substantial effect of channel morphology of individual river sections on breakup timing, it can be difficult to generalize breakup drivers among different rivers. The complex patterns observed demonstrate a need for additional analysis of spatial trends in breakup processes combined with field and modeling studies.

6.3. Future directions

The results presented in this paper represent only an initial analysis of the river ice measurements that can be derived from MODIS imagery. Detection of breakup mechanisms and event severity is of particular interest in current river ice research (Prowse et al., 2007). To this end, one possible related application of MODIS imagery is classification of thermal and mechanical breakup events. Several studies have predicted a trend towards more thermal breakup events and a corresponding decrease in event severity, yet more observations of breakup events are needed to confirm this outcome (e.g., Prowse et al., 2010).

To assess the applicability of this method for classification of breakup types, we identify and discuss the appearance of three primary types of breakup: thermal, mechanical and morphologically constrained. Thermal breakup is characterized by a decreased resisting force due to ice cover ablation and generally involves little-to-no ice jamming and flooding (low severity). In MODIS imagery, we hypothesize that thermal breakup appears as a slowly ablating ice surface (decreasing surface reflectance) where the transition from ice to mixed ice/water to open water occurs over a period of several days to weeks (Fig. 9a). The shift from ice to water is predominantly smooth and linear both in time and along the river.

In contrast, mechanical breakup is caused by a strong upstream force encountering significant downstream ice cover, often leading to ice jams and flooding (high severity). During mechanical breakup events, the ice cover is discontinuous and in motion, frequently resulting in open water in between ice-covered segments. Mechanical breakup viewed in MODIS imagery is likely distinguished by a fast transition from ice to water and discontinuous segments of ice-cover and open water (Fig 9b). Unlike in thermal breakup events, relatively high reflectance (non-melted) ice may be in contact with open water, and the location of open water reaches can vary from day to day.

Breakup progression in especially braided river reaches combines aspects of both mechanical and thermal breakups due to the differing channel morphology governing flow (Fig. 9c). First, there is generally an overall decrease in reflectance, indicating surface ice melting and weakening resistance. Ice then becomes concentrated on the main channels due to higher flow in the larger branches. Eventually, the main branches begin to break up, leading to discontinuous stretches of mixed ice/water and open water. At some point, water can flow through the open branches unimpeded by the presence of ice, though small areas of ice cover on outer braids can remain after most of the segment has broken up.

The differences in the appearance of breakup progression shown in Fig. 9 demonstrate that it may be possible to determine breakup type and event severity from MODIS imagery. The above assessment represents only an exploratory examination of the apparent signatures of mechanical and thermal breakup events on large, remote northern rivers. Thorough identification of breakup mechanisms would additionally require fieldwork and the incorporation of higher-resolution satellite imagery.

7. Summary and conclusions

The river ice breakup detection algorithm presented in this paper provides a useful new method of studying breakup at large scales and is sufficiently precise for robust analyses of spatial patterns in breakup timing. We identify several patterns that provide insight into possible drivers of breakup progression. Our results for the Mackenzie confirm a previously identified transition to earlier ice breakup in the Mackenzie Delta attributed to rising downstream temperatures and weakening ice resistance. Observed trends towards earlier upstream breakup and strong correlations between breakup initiation and overall breakup patterns suggest that earlier onset of breakup dominates breakup timing in Siberia. The complexity of the patterns observed emphasizes the need for further analysis of relationships between discharge, precipitation and breakup timing continuously along river. In the future, given the required ancillary datasets and a longer time series of MODIS imagery, this algorithm would be well suited for study of breakup mechanisms and the causes of observed trends towards earlier breakup. This method could also be used to assess breakup event type and severity, enabling further research on projected shifts towards more thermal breakup events. Finally, combining these spatial analyses with both hydrological and climate modeling approaches could further improve the understanding of the response of river ice to a warming Arctic.

Acknowledgments

We thank two anonymous reviewers for their useful comments on an earlier draft of this paper. T. Pavelsky's contributions were funded by NASA New Investigator Program Grant #NNX12AQ77G.

References

Ackerman, S., Frey, R., Strabala, K., Liu, Y., Gumley, L., Baum, B., & Menzel, P. (2010). *Algorithm theoretical basis document for discriminating clear-sky from cloud with MODIS (MOD35)*. Cooperative Institute for Meteorological Satellite Studies. Madison: University of Wisconsin.

Allen, G. H., & Pavelsky, T. M. (2015). Patterns of river width and surface area revealed by the satellite-derived North American River Width data set. *Geophysical Research Letters*, *42*, 395–402. http://dx.doi.org/10.1002/2014GL062764.Received.

Beltaos, S. (2003). Threshold between mechanical and thermal breakup of river ice cover. *Cold Regions Science and Technology*, *37*, 1–13. http://dx.doi.org/10.1016/S0165-232X(03)00010-7.

Beltaos, S., & Prowse, T. (2009). River-ice hydrology in a shrinking cryosphere. *Hydrological Processes*, *23*, 122–144. http://dx.doi.org/10.1002/hyp.7165.

Bennett, K. E., & Prowse, T. D. (2010). Northern hemisphere geography of ice-covered rivers. *Hydrological Processes*, *24*, 235–240. http://dx.doi.org/10.1002/hyp.7561.

Bernier, M., & Gauthier, Y. (2006). Monitoring the cryosphere using Radarsat-1 and SSM/I data: An overview of CRYSYS related accomplishments at INRS-ETE. *International geoscience and remote sensing symposium (IGARSS)* (pp. 1879–1882). http://dx.doi.org/10.1109/IGARSS.2006.485.

Bieniek, P. A., Bhatt, U. S., Rundquist, L. A., Lindsey, S. D., Zhang, X., & Thoman, R. L. (2011). Large-scale climate controls of interior Alaska river ice breakup. *Journal of Climate*, *24*, 286–297. http://dx.doi.org/10.1175/2010JCLI3809.1.

Bonsal, B. R., Prowse, T. D., Duguay, C. R., & Lacroix, M. P. (2006). Impacts of large-scale teleconnections on freshwater-ice break/freeze-up dates over Canada. *Journal of Hydrology*, *330*, 340–353. http://dx.doi.org/10.1016/j.jhydrol.2006.03.022.

Brown, R. D., & Mote, P. W. (2009). The response of northern hemisphere snow cover to a changing climate. *Journal of Climate*, *22*, 2124–2145. http://dx.doi.org/10.1175/2008JCLI2665.1.

Catchpole, A. J. W., & Moodie, D. W. (1974). Changes in the Canadian definitions of breakup-up and freeze-up. *Atmosphere*, *12*(1), 133–138.

Chaouch, N., Temimi, M., Romanov, P., Cabrera, R., Mckillop, G., & Khanbilvardi, R. (2014). An automated algorithm for river ice monitoring over the Susquehanna River using the MODIS data. *Hydrological Processes*, *28*, 62–73. http://dx.doi.org/10.1002/hyp.9548.

Cook, T. L., & Bradley, R. S. (2010). An analysis of past and future changes in the ice cover of two high-Arctic lakes based on synthetic aperture radar (SAR) and landsat imagery. *Arctic, Antarctic, and Alpine Research*, *42*(1), 9–18. http://dx.doi.org/10.1657/1938-4246-42.1.9.

De Rham, L. P., Prowse, T. D., & Bonsal, B. R. (2008). Temporal variations in river-ice breakup over the Mackenzie River Basin, Canada. *Journal of Hydrology*, *349*, 441–454. http://dx.doi.org/10.1016/j.jhydrol.2007.11.018.

Déry, S. J., Hernández-Henríquez, M. A., Burford, J. E., & Wood, E. F. (2009). Observational evidence of an intensifying hydrological cycle in Northern Canada. *Geophysical Research Letters*, *36*, 1–5. http://dx.doi.org/10.1029/2009GL038852.

Dey, B., Moore, H., & Gregory, A. F. (1977). The use of satellite imagery for monitoring ice break-up along the Mackenzie River, N.W.T. *Arctic*, *30*.

Duguay, C. R., Bernier, M., Gauthier, Y., & Kouraev, A. (2015). Remote sensing of lake and river ice. In M. Tedesco (Ed.), *Remote sensing of the cryosphere* (pp. 273–306). Chichester, UK: John Wiley & Sons.

Floyd, A. L., Prakash, A., Meyer, F. J., Gens, R., & Liljedahl, A. (2014). Using synthetic aperture radar to define spring breakup on the Kuparuk River, Northern Alaska. *Arctic*, *67*(4), 462–471.

Gatto, L. W. (1990). Monitoring river ice with landsat images. *Remote Sensing of Environment*, *32*, 1–16. http://dx.doi.org/10.1016/0034-4257(90)90094-3.

Gauthier, Y., Tremblay, M., Bernier, M., & Furgal, C. (2010). Adaptation of a radar-based river ice mapping technology to the Nunavik context. *Canadian Journal of Remote Sensing*, *36*, S168–S185 (SUPPL.).

Ginzburg, B. M., Polyakova, K. N., & Soldatova, I. I. (1992). Secular changes in dates of ice formation on rivers and their relationship with climate change. *Soviet Meteorology and Hydrology*, *12*, 57–64.

Goulding, H. L., Prowse, T. D., & Beltaos, S. (2009). Spatial and temporal patterns of break-up and ice-jam flooding in the Mackenzie Delta, NWT. *Hydrological Processes*, *23*, 2654–2670. http://dx.doi.org/10.1002/hyp.

Hall, D. K., Riggs, G. A., & Barton, J. S. (2001). *Algorithm theoretical basis document for the MODIS snow and sea ice mapping algorithms.* NASA Goddard Spaceflight Center.

Helsel, D. R., & Hirsch, R. M. (1992). *Statistical methods in water resources.* Amsterdam: Elsevier.

Hicks, F. E., Cui, W., & Ashton, G. (2008). Heat transfer and ice cover decay. In S. Beltaos (Ed.), *River ice breakup* (pp. 67–123). Highlands Ranch, CO: Water Resour. Publ.

Jeffries, M. O., Morris, K., & Kozlenko, N. (2005). Ice characteristics and remote sensing of frozen rivers and lakes. *Remote Sensing in Northern Hydrology: Geophysical Monograph Series*, *163*, 63–90. http://dx.doi.org/10.1029/163GM05.

Kropáček, J., Chen, F., Hoerz, S., & Hochschild, V. (2013). Analysis of ice phenology of lakes on the Tibetan Plateau from MODIS data. *The Cryosphere*, *7*, 287–301. http://dx.doi.org/10.5194/tc-7-287-2013.

Latifovic, R., & Pouliot, D. (2007). Analysis of climate change impacts on lake ice phenology in Canada using the historical satellite data record. *Remote Sensing of Environment*, *106*, 492–507. http://dx.doi.org/10.1016/j.rse.2006.09.015.

Lesack, L., Marsh, P., Hicks, F., & Forbes, D. (2014). Local spring warming drives earlier breakup in a large Arctic delta. *Geophysical Research Letters*, 1560–1566. http://dx.doi.org/10.1002/2013GL058761.

Magnuson, J., Robertson, D., Benson, B., Wynne, R., Livingstone, D., Arai, T., ... Vuglinski, V. (2000). Historical trends in lake and river ice cover in the northern hemisphere. *Science*, *289*, 1743–1746. http://dx.doi.org/10.1126/science.289.5485.1743.

Maslanik, J. A., & Barry, R. G. (1987). Lake ice formation and breakup as an indicator of climate change: potential for monitoring using remote sensing techniques. *The influence of climate change and climate variability on the hydrologic regime and water resources*, *168*.

Mermoz, S., Allain-Bailhache, S., Bernier, M., Pottier, E., Van Der Sanden, J. J., & Chokmani, K. (2014). Retrieval of river ice thickness from C-band PolSAR data. *IEEE Transactions on Geoscience and Remote Sensing*, *52*(6), 3052–3062. http://dx.doi.org/10.1109/TGRS.2013.2269014.

Nolan, M., Liston, G., Prokein, P., Brigham-Grette, J., Sharpton, V. L., & Huntzinger, R. (2002). Analysis of lake ice dynamics and morphology on Lake El'gygytgyn, NE Siberia, using synthetic aperture radar (SAR) and Landsat. *Journal of Geophysical Research*, *108*, 1–12. http://dx.doi.org/10.1029/2001JD000934.

Pavelsky, T. M., & Smith, L. C. (2004). Spatial and temporal patterns in Arctic river ice breakup observed with MODIS and AVHRR time series. *Remote Sensing of Environment*, *93*, 328–338. http://dx.doi.org/10.1016/j.rse.2004.07.018.

Peterson, B. J., Holmes, R. M., McClelland, J. W., Vörösmarty, C. J., Lammers, R. B., Shiklomanov, A. I., ... Rahmstorf, S. (2002). Increasing river discharge to the Arctic Ocean. *Science*, *298*, 2171–2173. http://dx.doi.org/10.1126/science.1077445 (December).

Prowse, T. D. (2001a). River-ice ecology. I: Hydrologic, geomorphic, and water-quality aspects. *Journal of Cold Regions Engineering*, *15*, 1–16.

Prowse, T. D. (2001b). River-ice ecology. II: Biological aspects. *Journal of Cold Regions Engineering*, *15*(1), 17–33.

Prowse, T., Bonsal, B. R., Duguay, C. R., & Lacroix, M. P. (2007). River-ice break-up/freeze-up: A review of climatic drivers, historical trends and future predictions. *Annals of Glaciology*, *46*, 443–451. http://dx.doi.org/10.3189/172756407782871431.

Prowse, T., Shrestha, R., Bonsal, B., & Dibike, Y. (2010). Changing spring air-temperature gradients along large northern rivers: Implications for severity of river-ice floods. *Geophysical Research Letters*, *37*, 1–6. http://dx.doi.org/10.1029/2010GL044878 (August).

Rawlins, M. A., Steele, M., Holland, M. M., Adam, J. C., Cherry, J. E., Francis, J. A., ... Zhang, T. (2010). Analysis of the Arctic system for freshwater cycle intensification: Observations and expectations. *Journal of Climate*, *23*, 5715–5737. http://dx.doi.org/10.1175/2010JCLI3421.1.

Sakai, T., Hatta, S., Okumura, M., Hiyama, T., Yamaguchi, Y., & Inoue, G. (2015). Use of Landsat TM/ETM + to monitor the spatial and temporal extent of spring breakup floods in the Lena River, Siberia. *International Journal of Remote Sensing*, *36*, 719–733. http://dx.doi.org/10.1080/01431161.2014.995271 (May).

Serreze, M. C., Barrett, A. P., Slater, A. G., Woodgate, R. a., Aagaard, K., Lammers, R. B., ... Lee, C. M. (2006). The large-scale freshwater cycle of the Arctic. *Journal of Geophysical Research: Oceans*, *111*, 1–19. http://dx.doi.org/10.1029/2005JC003424.

Shiklomanov, A. I., & Lammers, R. B. (2014). River ice responses to a warming Arctic—Recent evidence from Russian rivers. *Environmental Research Letters*, *9*, 035008. http://dx.doi.org/10.1088/1748-9326/9/3/035008.

Shiklomanov, A. I., Lammers, R. B., Rawlins, M. A., Smith, L. C., & Pavelsky, T. M. (2007). Temporal and spatial variations in maximum river discharge from a new Russian data set. *Journal of Geophysical Research: Biogeosciences*, *112*, 1–14. http://dx.doi.org/10.1029/2006JG000352 (December).

Shiklomanov, A. I., Lammers, R. B., & Vorosmarty, C. J. (2002). Widespread decline in hydrological monitoring threatens pan-Arctic research. *Eos*, *83*(2).

Smith, L. C. (2000). Trends in Russian Arctic river-ice formation and breakup, 1917 to 1994. *Physical Geography*.

Smith, L. C. (2002). Emerging applications of interferometric synthetic aperture radar (InSAR) in geomorphology and hydrology. *Annals of the Association of American Geographers*, *92*, 385–398. http://dx.doi.org/10.1111/1467-8306.00295 (March 2015).

Smith, L. C., Pavelsky, T. M., MacDonald, G. M., Shiklomanov, A. I., & Lammers, R. B. (2007). Rising minimum daily flows in northern Eurasian rivers: A growing influence of groundwater in the high-latitude hydrologic cycle. *Journal of Geophysical Research: Biogeosciences*, *112*. http://dx.doi.org/10.1029/2006JG000327.

Sobiech, J., & Dierking, W. (2013). Observing lake- and river-ice decay with SAR: Advantages and limitations of the unsupervised k-means classification approach. *Annals of Glaciology*, *54*(62), 65–72. http://dx.doi.org/10.3189/2013AoG62A037.

Unterschultz, K. D., van der Sanden, J., & Hicks, F. E. (2009). Potential of RADARSAT-1 for the monitoring of river ice: Results of a case study on the Athabasca River at Fort McMurray, Canada. *Cold Regions Science and Technology*, *55*(2), 238–248. http://dx.doi.org/10.1016/j.coldregions.2008.02.003.

Vermote, E. F., Kotchenova, S. Y., & Ray, J. P. (2011). MODIS surface reflectance user's guide. *MODIS land surface reflectance science computing facility*.

Vincent, F., Raucoules, D., Degroeve, T., Edwards, G., & Abolfazl Mostafavi, M. (2004). Detection of river/sea ice deformation using satellite interferometry: Limits and potential. *International Journal of Remote Sensing*, *25*, 3555–3571. http://dx.doi.org/10.1080/01431160410001688303 (December 2014).

Vuglinsky, V. S. (2002). Peculiarities of ice events in Russian Arctic rivers. *Hydrological Processes*, *16*, 905–913. http://dx.doi.org/10.1002/hyp.365 (May 2001).

Vuglinsky, V. S. (2006). Ice regime in the rivers of Russia, its dynamics during the last decades and possible future changes. In H. Saeki (Ed.), *Proc. of 18th IAHR international symposium on ice* (pp. 93–98).

Weber, F., Nixon, D., & Hurley, J. (2003). Semi-automated classification of river ice types on the peace river using RADARSAT-1 synthetic aperture radar (SAR) imagery. *Canadian Journal of Civil Engineering*, *30*, 11–27. http://dx.doi.org/10.1139/l02-073.

Wynne, R. H., & Lillesand, T. M. (1993). Satellite observation of lake ice as a climate indicator — Initial results from statewide monitoring in Wisconsin. *Photogrammetric Engineering & Remote Sensing*, *59*(6), 1023–1031.